Received: 27 January 2021 | Revised: 4 August 2021 | Accepted: 26 August 2021

DOI: 10.1111/vsu.13725

WILEY

CASE REPORT

Single-cut osteotomy for correction of a complex multiplanar deformity of the radius in a Shetland pony foal

Lorenz P. Schweinsberg DVM[1] | Anna Ehrle DVM, DECVS DECVSMR, MRCVS[1] | Uwe Schweinsberg DING[2] | Lucy Meehan CertAVP(VDI), DECVDI, MRCVS[3] | Andrea Noguera Cender DVM, DECVS[1] | Christoph J. Lischer DVM, DECVS, DECVDI (Large Animal)[1]

[1]Equine Clinic, Surgery and Radiology, Freie Universität Berlin, Berlin, Germany

[2]Ingenieurbüro Schweinsberg, Bochum, Germany

[3]VetCT, St John's Innovation Centre, Cambridge, UK

Correspondence
Lorenz P. Schweinsberg, Equine Clinic, Surgery and Radiology, Freie Universität Berlin, Berlin, Germany, Oertzenweg 19 b, 14 163 Berlin, Germany.
Email: lorenz.schweinsberg@fu-berlin.de

Abstract

Objective: To describe the surgical correction of a multiplanar deformity of the radius in a pony using a single-cut osteotomy.

Study design: Case report.

Animals: A 9-week-old male Shetland pony foal with a bodyweight of 47 kg.

Methods: The foal presented with a complex multiplanar deformity of the right radius. A 3-dimensional model of the bone was created based on computed tomography (CT) imaging. To correct the deformity, the cutting plane for a single-cut osteotomy was calculated following the mathematical approach described by Sangeorzan et al. After osteotomy, the bone was realigned and stabilized with two 4.5 locking compression plates (LCPs).

Results: Recovery from surgery was uneventful, and the foal remained comfortable. A CT exam 15 weeks after surgery revealed that diaphyseal deformities improved substantially in procurvatum (from 8° to 1°), varus (from 27° to 0°), and rotation (30° to 5°). The operated radius was 2.1 cm shorter than the left. Eighteen-month follow up confirmed a functionally and cosmetically acceptable outcome.

Conclusion: The single-cut osteotomy resulted in the successful correction of a multiplanar equine long-bone deformity with a favorable outcome in a Shetland pony.

Clinical significance: Single-cut osteotomy is an alternative surgical technique for the correction of complex diaphyseal long-bone equine deformities. Computed tomography data and the possibility of printing 3D models provides a significant advantage for rehearsing the procedure and for evaluating the correction that was achieved.

1 | INTRODUCTION

The etiology of bone deformities is multifactorial. Genetic or perinatal factors, including aberrant or incomplete ossification and periarticular laxity, and developmental factors like dietary imbalance, overload, or trauma, may play a role in long-bone misalignment progression.[1–7] Acquired causes, such as infection or fracture malunion, can also be involved.[1–7]

In small horse breeds, severe limb deformities are often associated with the complete ossification of the ulna or fibula (skeletal atavism).[1,8] Shetland ponies and miniature horses most frequently present with angular limb deformities but more complex bone deformations can occur.[1,2,8]

Complex limb deformities result from a combination of angular and torsional deviation in long bones.[2,9] Conservative management is usually unsuccessful in foals older than 3-6 months of age, especially in small horse breeds, which show a reduced growth potential compared with their larger counterparts.[2,10,11] Corrective surgical treatment for complex long-bone deformities described in equids includes osteotomy and ostectomy in the sagittal and frontal plane, and closing-wedge ostectomy.[12–16]

Single-cut osteotomies are also described in the human literature, mainly for treating fracture malunion.[17–23] A single-cut osteotomy is performed in the plane of maximal deformity, and correction is subsequently achieved by rotation and potentially translation of the opposing bone surfaces. The single-cut osteotomy's main advantage is the increased bone contact, which facilitates a stable fixation and accelerates bone healing.[23,24] This technique requires 3-dimensional planning based on computed tomography (CT) data, followed by mathematical analysis before the osteotomy plane can be determined. The realigned bone is stabilized using basic principles of long-bone plating.[18,23]

A single oblique-osteotomy has been described in a dog for the correction of an antebrachial deformity.[25] This is the first report of a single-cut osteotomy to correct a complex multiplanar deformity of a long bone in an equine patient, to the best of the authors' knowledge.

2 | MATERIALS AND METHODS

2.1 | History and clinical findings

A 9-week-old male Shetland pony foal (47 kg) was referred by an ambulatory veterinarian for assessment of a severe complex malformation of the right forelimb. Information regarding parturition and delivery were not available. On admission, the foal was bright, alert, and responsive with all vital parameters within normal limits. A severe deformity of the mid-radius consisting of varus, procurvatum (backward bending), and external rotation was present. Carpal valgus and hyperextension of the metacarpophalangeal joint were also present (Figure 1). The foal was weight bearing on all four limbs and was able to ambulate at walk, trot, and canter, but displayed

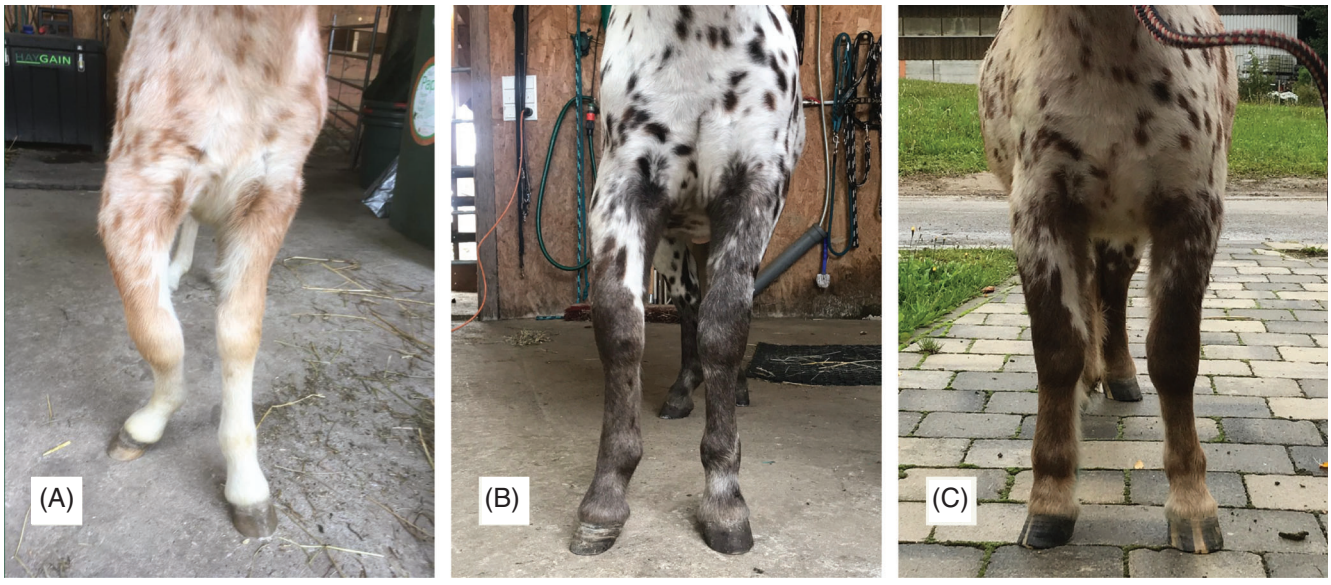

FIGURE 1 Development of the deformity of the right radius of the Shetland pony foal. A The 9-week-old male Shetland pony foal with lateral deviation of the radial diaphysis, carpus valgus, lateral rotation of the carpus and distal extremity and hyperextension of the metacarpophalangeal joint. B Shetland pony 6 weeks after corrective osteotomy, aged 4 months. C Shetland pony aged 10 months showing favorable cosmetic outcome 7 months postsurgery

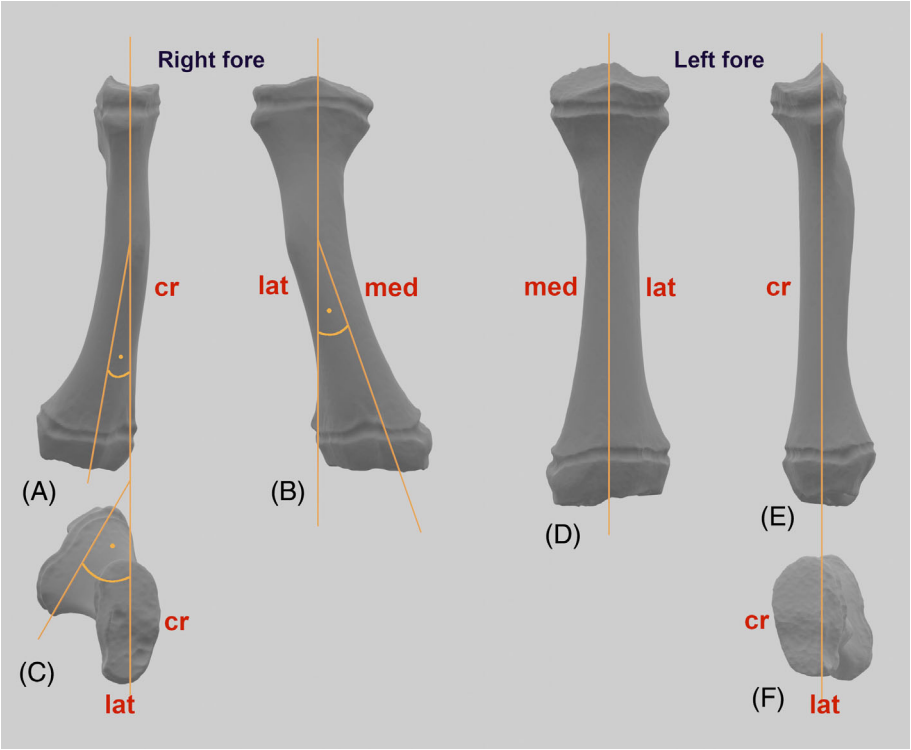

FIGURE 2 Three-dimensional reconstruction of the right (deformed) and left (undeformed) radius of the 9-week-old Shetland pony foal based on CT data. Lateral view (sagittal) A, E, dorsal view (frontal) B, D and proximal to distal (transverse) view C, F. Note the procurvatum (S = 8°; A), varus (C = 27°, B) and rotational (T = 30°; C) deformity of the right radius

what appeared to be a moderate mechanical lameness of the right forelimb.

2.2 | Diagnostic imaging

Following radiographic examination of the right radius in four planes (mediolateral, craniocaudal, craniomedial-caudolateral oblique, craniolateral-caudomedial oblique) CT was performed under general anesthesia in sternal recumbency (Aquilion LB, Canon). Computed tomography examination included both forelimbs from the scapula level to the distal phalanx, and the head and neck.

Computed tomography confirmed the diagnosis of a mid-diaphyseal varus (27°), procurvatum (8°), and an external rotational (30°) deformity of the right radius (Figure 2). There was no evidence for a fracture or associated callus formation. The left radius showed no significant deformation and was defined as undeformed. A moderate carpal valgus deformity of approximately 20° was also present in the right forelimb. Computed tomography data were further used to calculate the plane for a single-cut osteotomy.

2.3 | Presurgical planning

The definition of the deformity and the calculation for the location of the cutting plane are required to correct a complex long-bone deformity using a single cut osteotomy.[17,18]

TABLE 1 Deformation angles used for the characterization of a complex angular limb deformity and sign definitions for the calculation input[17,18]

Angles	Positive sign (+)	Negative sign (−)
C (frontal plane)	Varus	Valgus
S (sagittal plane)	Procurvatum	Recurvatum
T (transverse plane)	Internal rotation	External rotation

The CT data for both radii were transferred to free and open-source 3D software (Blender, Blender Foundation 2002, Amsterdam, Holland). The undeformed left radius was mirrored to be used as a template for the deformed right radius.[26] To define the deformity of the right radius, the deformation angles in the frontal (C), sagittal (S), and transverse (T) plane were determined (Figure 2) using the sign definitions outlined in Table 1.

Based on the measured values of the deformation angles C, S, and T, the true angle of deformity (A), orientation angle (α), and amount of rotation to correct all planes (β), rotation of the starting point (Φ), and inclination angle of the cut (θ) were subsequently calculated as described by Sangeorzan et al.[17,18] (Table 2).

The next step was to determine the plane of maximal deformity and the starting point for the osteotomy. The plane of maximal deformity is a transverse plane at the junction of the central axes of the proximal (z1 axis) and distal radius (z2 axis) (Figure 3A). The cutting plane of the

osteotomy is found by rotating the x1–y1 plane around the z1 axis about Φ and rotating the transformed x1–y1 plane around the y1 axis about θ (Figure 3B).[17,18] After completion of the osteotomy the distal bone segment is rotated about β. The rotation axis for angle β is the transformed z1 axis (vector **k** according to Sangeorzan et al.).[17,18]

A 3D model was printed (Formlabs Form 2) of the deformed (right) and the normal (left) radius to practice the procedure and to test the correction achieved through the calculated angles. Three strategic Kirschner wires (K wires) were inserted to provide orientation during surgery. Kirschner wire 1 was placed parallel to the distal radial physis in a latero-medial direction.

Kirschner wire 2 was inserted orthogonal to K wire 1 in the plane of maximal deformity. The rotation axis (K wire 3) is orthogonally located to the angle Φ and was placed at the point 15° lateral to K wire 2 (K wire 2: $\Phi - 90° + 15° = -44.6°$; K wire 3: $\Phi - 90° = -59.6°$; difference K wire 2 to K wire 3 = 15°) (Figures 4A-D and 3). With K wire 3 as starting point for the osteotomy, a template guided ascending cut at the angle of 43.8° (180° − θ) was performed (Figures 4C, D and 3).

Following osteotomy, the distal part of the radius was rotated in a medial direction (internal rotation) until the radius appeared straight in the frontal plane. The result was compared with the 3D model of the left, undeformed radius.

Two self-made stainless-steel templates were subsequently cut and sterilized to be used during surgery. The first template indicated an angle of 15° between K wire 2 and K wire 3 and the second template an angle of 43.8° (180° − θ). The templates were used to find the starting point (first template) and the inclination angle (second template) for the single-cut osteotomy (Figures 4A-D and 3).

TABLE 2 Input values (in degrees) and the results for the preoperative planning of a multiplanar angular limb deformity using the calculation method of Sangeorzan et al.[17,18]

Input	Results
C = 27 (varus +)	$A = 27.9$ (True angle of deformity)
S = 8 (procurvatum +)	$\alpha = 15.4$ (Orientation angle)
T = −30 (external rotation −)	$\beta = 40.7$ (Amount of rotation to correct all planes)
	$\Phi = -30.4$ (Rotation of the starting point)
	$\theta = 136.2$ (Inclination angle)
	Template 1: Angle betwen K wire 2 and K wire 3 = 15°
	Template 2: $180° - \theta = 43.8°$

2.4 | Surgery

For the elective procedure, flunixin meglumine (1.1 mg/kg intravenously [IV]), amoxicillin (10 mg/kg

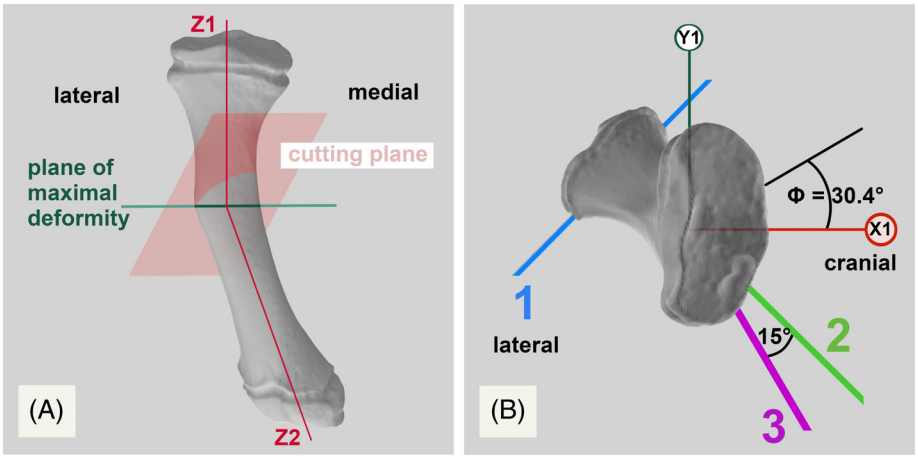

FIGURE 3 Demonstration of the required planes, axes, and pin placements for performing the single-cut osteotomy. A Frontal view of the deformed right radius with Z1 and Z2 axis, illustration of the plane of maximal deformity and the cutting plane. B Proximal to distal view of the deformed right radius. The point where angle θ is measured is defined by angle Φ, starting from the x1 axis in the plane of maximal deformity. Three strategic K wires were inserted to provide orientation during surgery. Kirschner wire 1 was placed parallel to the distal radial physis in a latero-medial direction. Kirschner wire 2 was inserted orthogonal to K wire 1 in the plane of maximal deformity (angle K wire 2 = $\Phi - 90° + 15° = -44.6°$). The rotation axis (K wire 3) is located orthogonally to the angle Φ and was placed at the point 15° (Angle between K wire 2 and K wire 3) lateral to K wire 2 ($\Phi - 90° = -59.6°$)

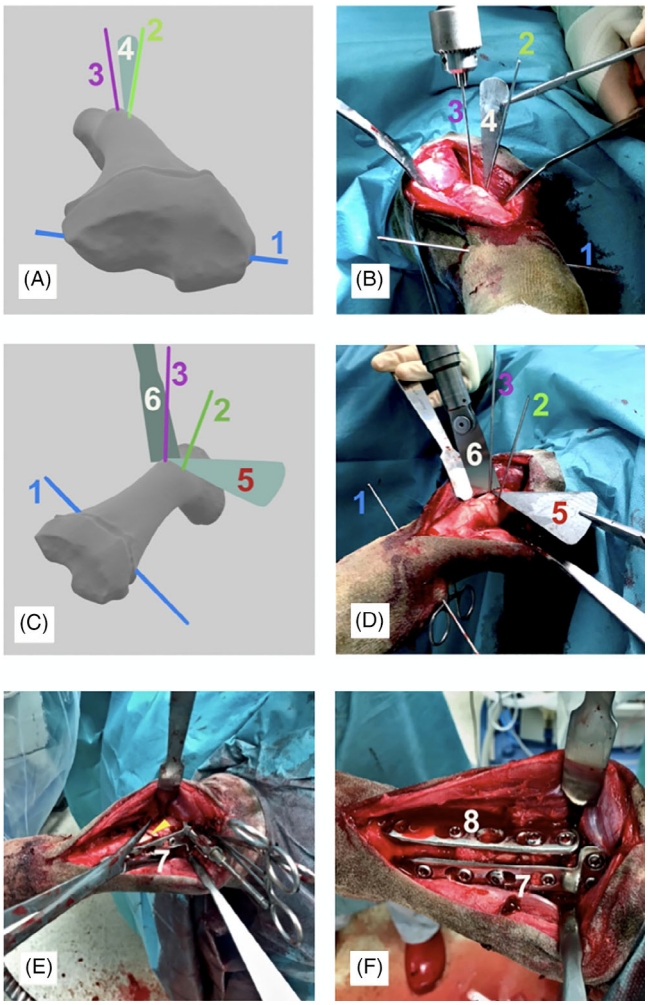

FIGURE 4 Pictures taken during the surgery with corresponding graphics to illustrate the procedure. A, B Three K wires are inserted in the radius to facilitate orientation during the surgical procedure. Kirschner wire (1) is positioned parallel and approximately 1 cm proximal to the distal radial physis in latero medial direction. Kirschner wire (2) is placed at an angle of 90° to K wire 1 at the plane of maximal deformity. Kirschner wire (3) is placed at the point 15° lateral to K wire 2 ($\Phi - 90° = -59.6°$). During surgery a sterile metal template (4) with a given angle of 15° was used to aid correct insertion of K wire 3. C, D A second metal template (5) with a given angle of 43.8° ($180° - \theta$) was prepared to determine the plane for the single-cut osteotomy of the radius. The tip of the template (5) was placed at the point of insertion of K wire 3. Osteotomy was performed with an oscillating saw (6). E, F Intraoperative views showing the fixation of the transected radius following osteotomy and realignment of the bone segments (yellow arrow indicating the osteotomy cut). The 4.5 mm 4-hole T-locking compression plate (LCP) (7) was placed first at the cranial aspect of the radius to secure reduction. A 4.5 mm 5-hole narrow LCP (8) was applied at the lateral aspect of the radius to provide increased stability

IV), and gentamycin sulfate (6.6 mg/kg IV) were administered preoperatively. The foal also received omeprazole (4 mg/kg orally, once daily) and sucralfate

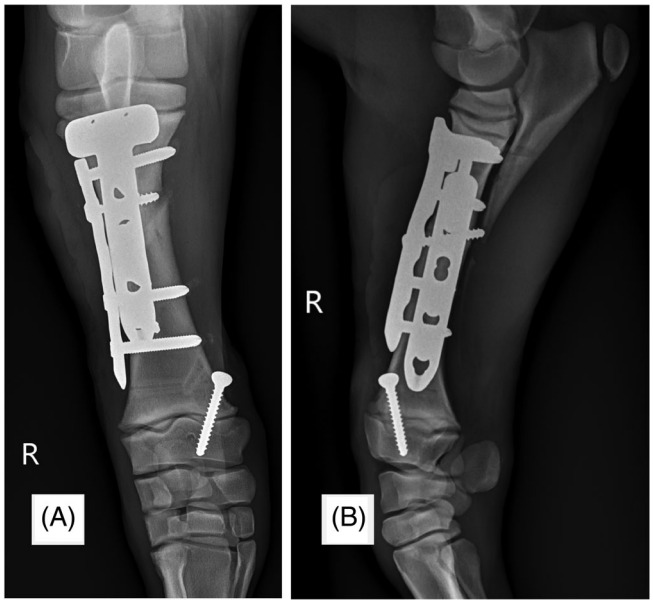

FIGURE 5 Radiographic outcome postsurgery. A Cranio-caudal, and B latero-medial radiographic projections of the right radius of the Shetland pony foal, post single-cut osteotomy for correction of a complex bone deformity

(12 mg/kg orally, twice daily) throughout hospitalization. Following induction of general anesthesia, the foal was placed in left lateral recumbency, the proximal right forelimb was aseptically prepared, and routine draping was applied.

A 20 cm skin incision was made for a cranial approach to the radius, and the extensor carpi radialis and common digital extensor muscles were separated bluntly. Three 1.5 mm K wires were inserted under fluoroscopic guidance to facilitate orientation and achieve correct alignment following osteotomy of the radius as described in the previous section (Figures 4A-D and 3).

Using the knowledge from the 3D model, the plane of maximal deformity was identified (crossing point from z1 axis upper bone segment and z2 axis lower bone segment). In the 3D model the bone had a convex apex, which was used for orientation, because this apex lies in the plane of maximal deformity.

Kirschner wire 1 was placed parallel and proximal to the distal radial physis in a latero-medial direction, this was achieved by using the aiming device and fluoroscopic guidance. Kirschner wire 2 was orthogonal to K wire 1, and a plate template was used to provide orthogonality for K wire 2 placement.

Based on the previously described calculations and definitions, a single-cut osteotomy of the right radius was performed with an oscillating saw (Colibri II; DePuy Synthes). Under fluoroscopic guidance, the distal part of

the right radius was subsequently rotated medially until the proximal physis was positioned parallel to the distal physis (K wire 1).

The alignment was maintained with bone reduction forceps, and standard double plating was used to stabilize the osteotomy. A 4.5-mm 4-hole T-locking compression plate (LCP) (Synthes T-LCP) was contoured and fixed to the cranial aspect of the right radius with 4.5 mm cortex screws and 5 mm locking head screws (Figure 5A). The third screw was a cortex screw, placed in lag fashion across the osteotomy plane. A second 4.5 mm 5-hole narrow LCP was positioned at the lateral aspect of the radius (Figure 5B). Positioning of the pins, correct alignment of the radius, the adequate positioning of the plates, and the length of the screws were determined and controlled with fluoroscopic guidance throughout the surgery.

Following surgical alignment of the radial diaphysis, the severe valgus deformity of the carpus became more apparent. For correction of the carpal valgus deformity a 4.5 mm transphyseal cortical screw 30 mm in length was placed as a position screw at the medial distal radius through a stab incision. Wound closure followed in three layers (continuous suture of the musculature (Ethicon, Vicryl USP 0), continuous suture of the subcutis (Braun, Monosyn USP 2/0), simple interrupted suture of the skin (Ethicon, Prolene USP 2/0)), the stab incision for the transphyseal screw was closed with simple interrupted sutures (Ethicon, Prolene USP 2/0). The two wounds were protected with a 2-layer bandage, which was kept in place using adhesive tape. Following 4 h surgery, hand-assisted anesthetic recovery was uneventful.

3 | RESULTS

The foal was fully weight bearing on the right forelimb throughout the postoperative period, and wound healing progressed without complications. Antimicrobial, anti-inflammatory therapy, and gastric protection were continued for 5 days (flunixin meglumine (1.1 mg/kg IV SID), amoxicillin (10 mg/kg IV TID), gentamycin sulfate (6.6 mg/kg IV SID), omeprazole (4 mg/kg SID), and sucralfate (12 mg/kg BID)). A medial extension (glue-on shoe, Dallmer) was attached to the right hoof to aid in correction of the carpal valgus deformity.

Fifteen weeks after surgery, the foal was admitted for repeated radiographic and CT examination as well as for the removal of the transphyseal screw. The pony was sound at walk and trot. Computer tomography identified a remaining deformity of 1° in the sagittal plane, 5° in the transverse plane. The frontal plane deformity was corrected completely. The carpal valgus deformity 15 weeks after surgery was about 5° and the hyperextension of the right metacarpophalangeal joint improved completely.

Telephone follow up with the owners at 18 months after surgery confirmed that the pony had developed normally with a favorable cosmetic and functional outcome (Figure 1).

4 | DISCUSSION

This report outlines the successful correction of a complex multiplanar deformity of the radius with a single-cut osteotomy in an equine patient. The technique was first described by D'Aubigne et al. for the correction of femoral deformities in human patients and later modified, improved, and applied to other long bones like the tibia by Sangeorzan et al.[17,18,27,28] The principle of the approach is based on the Euler theorem on rigid body dynamics. It shows that there is always an axis of rotation about which one bone segment can be rotated to align it with its counterpart.[29]

The procedure localizes the rotation axis of the cutting plane (vector **k**), orthogonal to the cutting plane, about which the distal bone segment can be rotated to align it with the proximal aspect of the bone. To define the deformity, the torsional component (T) can be measured directly (clinically or based on CT images) (Figure 2).[30] However, the deformity measurements in the frontal and sagittal plane may be distorted, especially when looking at radiographs.[31]

The single-cut osteotomy's main advantage is that accurate correction of a long-bone deformity can be achieved without bone loss. Direct bone contact facilitates a stable and rigid fixation that accelerates bone healing and most likely decreases the risk of complications like nonunion or implant failure.[23,24] A steep angle of transection often allows a lag screw to be placed across the osteotomy to enhance the correction's stability further. However, it should be noticed that the mathematical model is only useful if there is a torsional component to a complex long-bone deformity. A mild torsional component combined with a severe angular limb deformity results in a very steep osteotomy and makes the surgery more difficult.[25] The 4.5 mm T-LCP used for osteotomy stabilization in the described case has previously been applied in proximal tibia fractures in foals and has the advantage that several screws can be inserted in a short segment of bone.[32] The plate's T-part also fitted perfectly to the dorsal aspect of the radius, which was useful for controlling rotational alignment during surgery.

The single-cut osteotomy might potentially be less demanding than a wedge ostectomy. It is challenging to determine the accurate position for the second cut of a wedge in complex multiplanar deformities once the bone is divided. Overcorrection or undercorrection of the deformity or shortening of the bone may be introduced.[24] The step-ostectomy in the sagittal plane is presently the preferred technique as angular and rotational deformities can be corrected in one procedure. Good interfragmentary compression can be achieved using lag screws across the vertical saw cut.[2] However, in this case, it might have been challenging, if not impossible, to remove wedges to correct rotational and procurvatum deformity without introducing significant weakening of the bone. Provided the exact plane for the single-cut osteotomy is identified correctly, only one cut is required.

Careful presurgical planning is crucial for the success of the single-cut osteotomy. Miscalculation can easily result in the inadequate correction of a complex long-bone deformity.[17,18]

For combined angular and rotational deformities of long bones in humans, the deformation angles, including the frontal, sagittal and transverse deformity as well as the true angle of deformity, can be calculated based on two radiographs (lateral and anterior–posterior projections) only.[33] Another study demonstrated that increasing torsion interferes with radiographic measurements, particularly in the frontal plane deformity.[31] For the described case's presurgical planning, the authors felt that it was highly advantageous to determine the angles of the deformity based on CT data.[34] The determination of the angles in a combined torsional and angular deformity is not particularly easy to perform because the torsional deformity influences the angular deformity.

The 3D software (Blender 2.83.2, www.blender.org) facilitates the accurate measurement of the angles required for performing the surgery with the additional option to simulate the osteotomy and immediately verify the correction virtually. The contralateral bone as a reconstruction template for 3D preoperative planning of complex corrective osteotomies has been validated in the tibia in man.[26] Similar data for the equine radius are not available but the 3D reconstruction of the left, undeformed radius was a valuable aid during preoperative planning. A step-by-step guide for calculating the single-cut osteotomy, a manual geometrical calculation tool, and an automatic genetic algorithm framework is also available for human patients.[23,33] However, to test the graphical approach, we had to follow the calculations of Sangeorzan et al.

A limitation of this case report is its single-case character and the small size and low bodyweight of the patient. However, we believe that this technique can be used in larger foals or ponies, if the plane of deformity is in the mid diaphyseal region. Double plating and the use of the appropriate LCP technique can provide stability for oblique long-bone fractures in equids up to 300-400 kg in bodyweight.[35] Our recommendation is to perform the calculation first and observe the location and angle of the cut, and what the opportunity provided for fixation would be, prior to moving on to consider other types of osteotomies.

Another limitation is the correct measurement of the deformation angles S, C, and T, because no validated technique is available. Inaccurate measurements would affect the accuracy of the calculated angle but CT data and the skills to use 3D software might improve the quality of these measurement.

In future cases we would perform the surgery with a 3D printed cutting guide. After determining the cutting plane, it would be possible to create such a cutting guide using the 3D software. When we planned and performed the surgery there was no option to create such a cutting guide and so we used the strategic pins as orientation during surgery. An individual 3D cutting guide that fits the deformed bone exactly could potentially facilitate the procedure and might increase its accuracy.[20,22]

As an additional benefit we created a supplementary tool for the calculations together with a definition of the sign rules (http://osteotomytool.de). For this tool the angles (C), (S) and (T) are needed. The results are calculated using the formula published by Sangeorzan et al.[17,18] The sign rules must be considered.

We strongly recommend testing the osteotomy in a 3D model before performing the surgery on a patient.

The reported case gives a detailed explanation of a single-cut osteotomy with a favorable clinical outcome. To date, the correction of complex multiplanar limb deformities in equine patients is considered complicated surgery with a guarded to fair prognosis for athletic activity.[2,14] Additional reports of single-cut osteotomies in large animal cases are needed to determine their limitations and potential contributions for successful outcomes in these species.

ACKNOWLEDGMENTS

The authors would like to thank Professor Peter Böttcher for the help with 3D printing of the bone model and the referring veterinary surgeons for sending the case.

CONFLICT OF INTEREST

The authors declare no conflicts of interest related to this review.

AUTHOR CONTRIBUTIONS

Schweinsberg LP, DVM, Ehrle A, DVM, DECVS, DECVSMR, MRCVS, Noguera Cender A, DVM, DECVS, and Lischer CJ, DVM, DECVS, DECVDI (Large Animal): Actively involved in managing the case. Meehan L, BVSc, MSc, CertAVP(VDI), DipECVDI, MRCVS, European Specialist in Veterinary Diagnostic Imaging (Large Animal): Evaluated the computed tomographic study. Schweinsberg U, DING.: Mainly responsible for the mathematical calculations. All authors contributed to the preparation of the manuscript.

REFERENCES

1. Rafati N, Andersson LS, Mikko S, et al. Large deletions at the SHOX locus in the pseudoautosomal region are associated with skeletal atavism in Shetland ponies. *G3 (Bethesda)*. 2016;6:2213-2223.
2. Bischofberger AS, Auer J. Angular limb deformities. In: Auer JA, Stick JA, eds. *Equine Surgery*. 5th ed. Saunders; 2018:1471-1490.
3. McIlwraith CW. Incomplete ossification of carpal and tarsal bones in foals. *Equine Vet Educ*. 2003;15:79-81.
4. Witte S, Hunt R. A review of angular limb deformities. *Equine Vet Educ*. 2009;21:378-387.
5. Levine DG. The normal and abnormal equine neonatal musculoskeletal system. *Vet Clin North Am Equine Pract*. 2015;31:601-613.
6. Coleman MC, Whitfield-Cargile C. Orthopedic conditions of the premature and dysmature foal. *Vet Clin North Am Equine Pract*. 2017;33:289-297.
7. Sprinkle FP, Crowe MW. In utero fractures in foals. *Mod Vet Pract*. 1984;65:37.
8. Tyson R, Graham JP, Colahan PT, Berry CR. Skeletal atavism in a miniature horse. *Vet Radiol Ultrasound*. 2004;45:315-317.
9. Gladbach B, Pfeil J, Heijens E. Correction of leg deformities. Definition, estimation and realignment of axis deviation and misalignment. *Orthopade*. 1999;28:1023-1033.
10. Metzger J, Rau J, Naccache F, Bas Conn L, Lindgren G, Distl O. Genome data uncover four synergistic key regulators for extremely small body size in horses. *BMC Genomics*. 2018;19:492.
11. Heck L, Sanchez-Villagra MR, Stange M. Why the long face? Comparative shape analysis of miniature, pony, and other horse skulls reveals changes in ontogenetic growth. *PeerJ*. 2019;7:e7678.
12. White KK. Diaphyseal angular deformities in three foals. *J Am Vet Med Assoc*. 1983;182:272-279.
13. Fretz PB, McIlwraith CW. Wedge osteotomy as a treatment for angular deformity of the fetlock in horses. *J Am Vet Med Assoc*. 1983;182(3):245-250.
14. Epp TL. Step ostectomy as a treatment for varus deformity of a metatarsophalangeal joint in a 4.5-month-old colt. *Can Vet J*. 2007;48:519-521.
15. Getman L. Surgical treatment of severe, complex limb deformities in horses. *Equine Vet Educ*. 2011;23:386-390.
16. Radtke A, Morello S, Muir P, Arnoldy C, Bleedorn J. Application of computed tomography and stereolithography to correct a complex angular and torsional limb deformity in a donkey. *Vet Surg*. 2017;46:1131-1138.
17. Sangeorzan BJ, Sangeorzan BP, Hansen ST Jr, Judd RP. Mathematically directed single-cut osteotomy for correction of tibial malunion. *J Orthop Trauma*. 1989;3:267-275.
18. Sangeorzan BP, Judd RP, Sangeorzan BJ. Mathematical analysis of single-cut osteotomy for complex long bone deformity. *J Biomech*. 1989;22:1271-1278.
19. Gürke L, Strecker W, Martinoli S. Graphical analysis and operative technique of single-cut osteotomy for complex femur deformities. *Unfallchirurg*. 1999;102:684-690.
20. Dobbe JG, Pre KJ, Kloen P, Blankevoort L, Streekstra GJ. Computer-assisted and patient-specific 3-D planning and evaluation of a single-cut rotational osteotomy for complex long-bone deformities. *Med Biol Eng Comput*. 2011;49:1363-1370.
21. Dobbe JGG, du Pre KJ, Blankevoort L, Streekstra GJ, Kloen P. Computer-assisted oblique single-cut rotation osteotomy to reduce a multidirectional tibia deformity: case report. *Strategies Trauma Limb Reconstr*. 2017;12:115-120.
22. Imhoff FB, Schnell J, Magaña A, et al. Single cut distal femoral osteotomy for correction of femoral torsion and valgus malformity in patellofemoral malalignment-proof of application of new trigonometrical calculations and 3D-printed cutting guides. *BMC Musculoskelet Disord*. 2018;19:215.
23. Carrillo F, Roner S, von Atzingen M, et al. An automatic genetic algorithm framework for the optimization of three-dimensional surgical plans of forearm corrective osteotomies. *Med Image Anal*. 2019;2:101598.
24. Youngman J, Raptis D, Al-Dadah K, et al. An accurate method of determining a single-plane osteotomy to correct a combined rotational and angular deformity. *Strategies Trauma Limb Reconstr*. 2015;10:35-39.
25. Kim SY, Snowdon KA, DeCamp CE. Single oblique osteotomy for correction of antebrachial angular and torsional deformities in a dog. *J Am Vet Med Assoc*. 2017;251:333-339.
26. Schenk P, Vlachopoulos L, Hingsammer A, Fucentese SF, Fürnstahl P. Is the contralateral tibia a reliable template for reconstruction: a three-dimensional anatomy cadaveric study. *Knee Surg Sports Traumatol Arthrosc*. 2018;26:2324-2331.
27. Merle d'Aubigné R, Descamps L. L'ostéotomie plane oblique dans la correction des deformations des membres. *Bull Mem Arch Chir*. 1952;8:271-276.
28. Merle d'Aubigné R, Vaillant J. Correction simultanée des angles d'inclinaison et de torsion du col fémoral par l'ostéotomie plane oblique. *Rev Chir Orthop*. 1961;47:94-103.
29. Euler L. Formulae generales pro translatione quacunque corporum rigidorum. *Novi commentarii academiae scientiarum petropolitanae*. 1776;20:189-207.
30. Jakob R, Haertel M, Stussi E. Tibial torsion calculated by computerised tomography and compared to other methods of measurement. *J Bone Joint Surg*. 1980;62:238-242.
31. Piras LA, Peirone B, Fox D. Effects of antebrachial torsion on the measurement of angulation in the frontal plane: a cadaveric radiographic analysis. *Vet Comp Orthop Traumatol*. 2012;25:89-94.
32. Lischer C, Rossignol F, Watkins JP. AOTK system innovations. 2018.

33. Paccola CA. A simplified way of determining the direction of a single-cut osteotomy to correct combined rotational and angular deformities of long bones. *Rev Bras Ortop*. 2011;46:329-334.
34. Meola SD, Wheeler JL, Rist CL. Validation of a technique to assess radial torsion in the presence of procurvatum and valgus deformity using computed tomography: a cadaveric study. *Vet Surg*. 2008;37:525-529.
35. Watkins PW, Glass KG, Kümmerle JM. Radius and ulna. In: Auer JA, Stick JA, eds. *Equine Surgery*. 5th ed. Saunders; 2018:1675-1685.

How to cite this article: Schweinsberg LP, Ehrle A, Schweinsberg U, Meehan L, Noguera Cender A, Lischer CJ. Single-cut osteotomy for correction of a complex multiplanar deformity of the radius in a Shetland pony foal. *Veterinary Surgery*. 2022;51(1):148-156. doi:10.1111/vsu.13725